

Infrared and NMR Spectroscopic Studies of n-Alkanethiols Chemically Grafted on Dimethylzinc-Modified Silica Surfaces

V. Boiadjev,[†] A. Blumenfeld,[†] J. Gutow,[‡] and W. T. Tysoe^{*,†}

Department of Chemistry and Laboratory for Surface Studies, University of Wisconsin–Milwaukee, Milwaukee, Wisconsin 53211 and Department of Chemistry, 800 Algoma Boulevard, University of Wisconsin–Oshkosh, Oshkosh, Wisconsin 54901

Received January 31, 2000. Revised Manuscript Received May 26, 2000

Transmission infrared and solid-state nuclear magnetic resonance (NMR) spectroscopies are used to study the surface species formed by sequential reaction of hydroxylated, high-surface-area silica with dimethylzinc (DMZ) and n-alkanethiols of various chain lengths. Reaction of DMZ forms mainly surface methylzinc species. These convert to Zn-bound ethanethiolate surface species by reaction with ethane thiol, evolving nearly identical amounts of methane at each step. Temperature-dependent infrared spectra of these surface thiolate species reveal that they are stable in air and aqueous environments and up to about 400 K in vacuo. The major gas-phase products identified during annealing are diethyl sulfide and ethylene. Longer-chain n-alkanethiols (up to C₁₆) are reacted in benzene solutions and the modified silica powders are characterized by transmission infrared and solid-state NMR spectroscopies. The spectroscopic data demonstrate that the alkanethiolate chains retain their integrity and bind to the surface via the sulfur atom with their “tails” away from the surface. High thiolate coverages (similar to those of well-characterized self-assembled monolayers of thiols on gold and trichlorosilanes on silicon) are obtained in the case of shorter hydrocarbon chains. Carbon–hydrogen–nitrogen analyses and electron microprobe elemental analyses reveal that the density of the thiolate layer decreases with increasing chain length. This is attributed to the highly irregular surface geometry and may be avoided by using planar substrates, thus providing a novel strategy for self-assembly of organic molecules on various hydroxylated surfaces.

Introduction

During the past few years, increasing attention has focused on developing new strategies for surface modification of silicon^{1–4} and various oxide substrates by deposition of thin organic and inorganic films.⁵ Surfaces such as alumina, silica, zeolites, and transition metal oxides are often naturally terminated by hydroxyl groups. Other surfaces such as silicon and polyethylene may be pretreated to hydroxylate them.^{6,7} A potentially attractive route for modifying these surfaces is to react these acidic terminal hydroxyl groups with organometallic compounds (usually metal alkyls) to produce a layer of reactive organometallic intermediates.^{8–10} These can subsequently react with another reagent containing

an acidic hydrogen atom (H₂O, NH₃, H₂S). This strategy is well developed for organometallic chemical vapor deposition and atomic-layer growth of III–V and II–VI inorganic thin films.^{10–19}

Chemically grafting hydrocarbon chains on the hydroxylated substrates is a first step toward designing organic surface structures. Our earlier studies have shown that sequential chemical vapor deposition of trimethylaluminum and methanol on hydroxylated alumina gave rise to surface methoxy species. These readily hydrolyzed upon exposure to air or water.²⁰ In a subsequent study,²¹ it was shown that the problem of

* To whom correspondence should be addressed.

[†] University of Wisconsin–Milwaukee.

[‡] University of Wisconsin–Oshkosh.

(1) Feng, W.; Miller, B. *Langmuir* **1999**, *15*, 3152.

(2) Boukherroub, R.; Morin, S.; Bensebaa, F.; Wayner, D. D. M. *Langmuir* **1999**, *15*, 3831.

(3) Bergerson, W. F.; Mulder, I. A.; Hsung, R. P.; Zhu, X.-Y. *J. Am. Chem. Soc.* **1999**, *121*, 454 and references therein.

(4) Ellison, M. D.; Hamers, R. J. *J. Phys. Chem. B* **1999**, *103*, 6243.

(5) Ulman, A. *Introduction to Ultrathin Organic Films: From Langmuir Blodgett to Self-Assembly*; Academic: San Diego, CA, 1991.

(6) Nuzzo, R. G.; Smolinsky, G. *Macromolecules* **1984**, *17*, 1013.

(7) Rasmussen, J. R.; Stedronsky, E. R.; Whitesides, G. M. *J. Am. Chem. Soc.* **1977**, *99*, 4736.

(8) George, S. M.; Ott, A. W.; Klaus, J. W. *J. Phys. Chem.* **1996**, *100*, 13121.

(9) Soto, C.; Wu, R.; Bennett, D. W.; Tysoe, W. T. *Chem. Mater.* **1994**, *6*, 1705.

(10) Soto, C.; Boiadjev, V.; Tysoe, W. T. *Chem. Mater.* **1996**, *8*, 2359.

(11) Schlyer, D. J.; Ring, M. A. *J. Electrochem. Soc.* **1977**, *124*, 569.

(12) DenBaars, S. P.; Maa, B. Y.; Dapkus, P. D.; Danner, A. D.; Lee, H. C. *J. Cryst. Growth* **1986**, *77*, 188.

(13) Larsen, C. A.; Buchan, N. I.; Stringfellow, G. B. *Appl. Phys. Lett.* **1988**, *52*, 480.

(14) Tsang, W. T.; Miller, R. C. *Appl. Phys. Lett.* **1986**, *48*, 1288.

(15) Manasevit, H. M.; Hewitt, W. B.; Nelson, A. J.; Mason, A. R. *J. Electrochem. Soc.* **1989**, *136*, 3070.

(16) Manasevit, H. M. *J. Cryst. Growth* **1972**, *13/14*, 306.

(17) Hua, T. H.; Armgath, M. *J. Electron. Mater.* **1987**, *16*, 27.

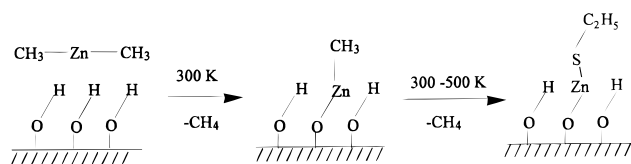
(18) Armitage, D. N.; Yates, H. M.; Williams, J. O.; Cole-Hamilton, D. J.; Patterson, I. L. *J. Adv. Mater. Opt. Electron.* **1992**, *1*, 43.

(19) Fujita, S.; Isemura, M.; Sakamoto, T.; Yoshimura, N. *J. Cryst. Growth* **1988**, *86*, 263.

(20) Boiadjev, V.; Tysoe, W. T. *Chem. Mater.* **1998**, *10*, 334.

(21) Boiadjev, V.; Tysoe, W. T. *Chem. Mater.* **1998**, *10*, 1141.

Scheme 1



hydrolysis could be eliminated by reacting the hydroxylated alumina surface with dimethylzinc (DMZ) and ethanethiol (EtSH). In the first step, the surface is covered mainly with the reactive methylzinc surface intermediates, which further react with ETSH to form surface thiolate species (Scheme 1).

In this study, this method is extended to growing films on silica, both in the vapor and from solution, with the ultimate goal of preparing self-assembled monolayers on planar surfaces. The main advantage of using powder substrates is their high surface area, which furnishes sufficiently strong signals to be studied by solid-state nuclear magnetic resonance (NMR) and transmission infrared spectroscopies. The main disadvantage is their surface irregularity, which does not permit self-assembly of the thiolate chains.

Experimental Section

Silica Sample Preparation. Reagent-grade silica (G. Frederick Smith Chemical Co.: Columbus, OH) was ground using a mortar and pestle^{20,21} and sequentially treated with DMZ and alkanethiol in benzene solution or pressed into a self-supported pellet (0.0132 g/cm², 25 500 pounds per square inch) for chemical vapor deposition experiments. Silica pellets for the *chemical vapor deposition* experiments were placed in an evacuable infrared cell that has been described in detail elsewhere.^{22,23} DMZ was synthesized as described earlier²¹ by reacting 0.05 mol anhydrous ZnCl₂ (EM Science, 98%) with 0.1 mol of trimethylaluminum (Aldrich Chemical Co., 97%). Its purity was verified by infrared spectroscopy. EtSH (Acros, 97%) was used after purification using four freeze-pump-thaw cycles.

Liquid-Phase Deposition. Films were grown from benzene solution in a nitrogen-filled glove box using a quartz vessel under constant stirring by a magnetic stirrer. EtSH (97%), 1-butanethiol (99+%), 1-octanethiol (97+%), 1-dodecanethiol (99+%, GC), and *n*-hexadecyl mercaptan (tech. 92+%) were from Acros, Fisher Scientific and used as received. Deuterated water (D₂O, 99 at. % D, Aldrich Chemical Co.) was used to deuterate unreacted hydroxyl groups remaining on the silica surface after the DMZ/butanethiol treatment by mixing with the modified powder and annealing at 400 K in vacuo for 1 h. The deuterated powder was then sealed in a glass tube under vacuum and loaded into the NMR spinner in a nitrogen-filled glove box to avoid exchange with the moisture in the air. Other samples for NMR experiments were prepared in air shortly after the completion of the vacuum-drying step.

Instrumentation. Small samples (~3 mg each) of the modified powders were precisely weighed ($\pm 1 \mu\text{g}$) and burned in the furnace of an EA 1110 CHN (carbon-hydrogen-nitrogen) elemental analyzer (CE Instruments).

Samples for the EDS electron microprobe analysis (using an energy-dispersive X-ray spectrometer) were prepared in air by pressing the treated powder onto a conductive carbon adhesive tape for scanning electron microscopy (Ted Pella).

Transmission infrared spectra were recorded using a Perkin-Elmer Fourier transform infrared spectrometer using a DTGS detector at a resolution of 4 cm⁻¹, accumulating 80 scans in the case of chemical vapor deposition experiments and at

resolution of 2 cm⁻¹ and 400 scans in the case of samples treated in benzene solution.

All NMR experiments were performed at room temperature under magic-angle spinning (MAS) conditions in a 11.7 T static field with a Bruker DRX-500 spectrometer equipped with a Doty 5-mm high-speed MAS probe. The spinning rates were varied between 4 and 13 kHz. The Hartmann-Hahn condition ($\omega_1^{\text{H}} - \omega_1^{\text{X}} = \pm n\omega_r$, where $\omega_r/2\pi$ is a spinning rate and X = ¹³C or ²⁹Si) for cross-polarization was adjusted before each experiment with fixed power levels in the proton channel (≈ 30 kHz for cross-polarization, ≈ 65 kHz for a 90° pulse, and ≈ 50 kHz for high-power decoupling). In most cases, the dipolar sideband with $n = -1$ was chosen. The number of accumulations for ¹H-¹³C CP MAS experiments progressively increased from 400 to 10 000 for increasing numbers of carbons in the thiol chain from 2 to 16. The ¹H-²⁹Si CP MAS spectra were obtained after 200–500 accumulations. The relaxation delay was 4 s in all experiments. All chemical shifts were referred to external ¹³C [solid adamantane, 37.7 and 28.6 parts per million (ppm) from Trimethylsilane (TMS)] and ²⁹Si (solid kaolinite, -91.5 ppm from TMS) standards.

The ¹H-²⁹Si CP dynamics were measured at a low spinning rate of 4 kHz with variable contact time τ_{CP} duration (from 0.2 to 25 ms). The spectra were deconvoluted into two (or three) lines with a Gaussian line shape function and their integrated intensities were fitted with a three-parameter standard equation:²⁴

$$I(\tau_{\text{CP}}) = I_0 \frac{\exp\left(-\frac{\tau_{\text{CP}}}{T_{1\rho}^{\text{H}}}\right) - \exp\left(-\frac{\tau_{\text{CP}}}{T_{\text{CP}}}\right)}{1 - \frac{T_{\text{CP}}}{T_{1\rho}^{\text{H}}}} \quad (1)$$

where $T_{1\rho}^{\text{H}}$ is a proton spin-lattice relaxation time in the rotating frame, T_{CP} is a time constant of the polarization transfer from protons to silicons, and I_0 is a theoretical maximum intensity.

Results and Discussion

Reaction of Hydroxylated Silica Surfaces with DMZ in Vacuo. The infrared features of the silica powders were identical to those found by others.^{22,23,25–28} Methane was detected in the gas-phase infrared spectra upon exposing the prehydroxylated silica pellets to a saturated vapor of DMZ at room temperature (~ 344 Torr) for ~ 20 min. According to Morrow and McFarlane,²³ this is the time necessary to completely react with all accessible surface silanols. This is confirmed by a significant decrease of infrared absorption intensity in the region of surface -OH stretching modes, which remained constant for larger DMZ exposures. A typical spectrum of methylzinc species remaining on the surface of the silica pellets after evacuation at room temperature is displayed in Figure 1. The C-H stretching modes at 2964 and 2916 cm⁻¹ with a shoulder at 2852 cm⁻¹ closely resemble the spectrum of the methylzinc surface species on alumina.²¹ Because of the very intense absorption by the silica Si-O lattice modes near and

(24) Mehring, M. *Principles of High-Resolution NMR in Solids*; Springer Verlag: Berlin, 1983.

(25) Hair, M. L. *Infrared Spectroscopy in Surface Chemistry*; Marcel Dekker: New York, 1967.

(26) Kiselev, A. V.; Lygin, V. I. *Infrared Spectra of Surface Compounds*; Wiley: New York, 1975.

(27) Morrow, B. A. In *Spectroscopic Analysis of Heterogeneous Catalysts, Part A: Methods of Surface Analysis*; Fierro, J. L. G., Ed.; Elsevier: Amsterdam, 1990; Chapter 3.

(28) Silverstein, R. M.; Bassler, G. C.; Morrill, T. C. *Spectroscopic Identification of Organic Compounds*; Wiley: New York, 1991.

(22) Tripp, C. P.; Hair, M. L. *Langmuir* **1992**, *8*, 1961.

(23) Morrow, B. A.; McFarlane, A. J. *Langmuir* **1991**, *7*, 1695.

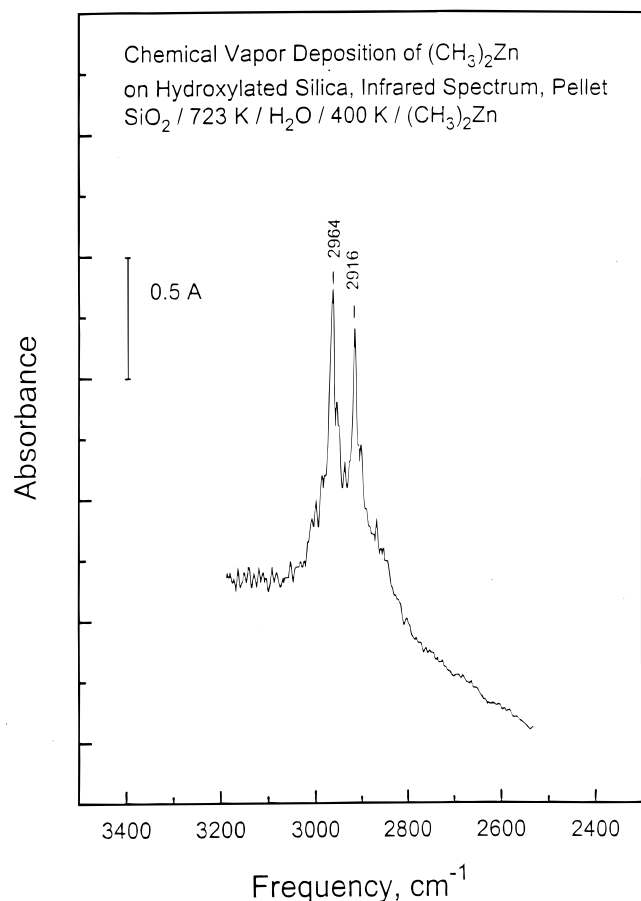


Figure 1. Infrared spectrum of DMZ-modified silica pellet displaying the C–H stretching modes of the surface species remaining after evacuation at room temperature.

below 1300 cm^{-1} , the low-intensity bending modes of these methylzinc species, which appear at ~ 1274 and $\sim 1180\text{ cm}^{-1}$ on alumina,²¹ are not observed on silica.

Reaction of Hydroxylated Silica with DMZ in Benzene. Similar results are obtained by reaction of DMZ with a silica powder suspended in benzene (Figure 2). The first spectrum [Figure 2 (a)], obtained from a thin layer deposited on the window of the small infrared cell, is typical of prehydroxylated silica before DMZ treatment.^{22,23,25–28} Substantial methane evolution is observed upon dropwise addition of the DMZ solution to prehydroxylated silica suspended in $\sim 5\text{ mL}$ of benzene. It continues at a slower rate even after all the reactant solution has been added. The presence of excess of DMZ, after this first deposition step, is verified in the filtrate by the significant methane evolution when neutralized with isobutanol before its disposal.

The spectrum of this sample obtained after thorough washing in benzene is shown in Figure 2 (b) where the C–H stretching modes at 2967 , 2918 , and 2854 cm^{-1} closely resemble the methylzinc surface species *vapor deposited* on silica as discussed above (Figure 1). The peak at 3016 cm^{-1} is due to residual methane. The appearance of these methylzinc surface species is accompanied by a very pronounced decrease in the intensity of the modes due to surface silanols. The ratio of the baseline-corrected integrated absorbencies between 3768 and 3121 cm^{-1} due to surface OH groups [Figure 2(a) and 2(b)], also corrected for sample thickness, is

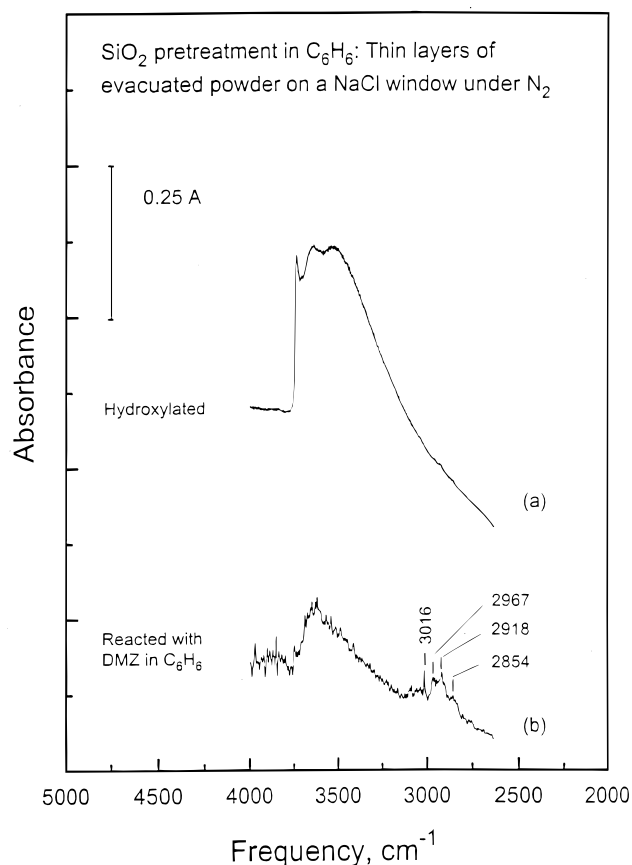


Figure 2. Infrared spectra of thin-layer silica powder showing the O–H and C–H stretching region: (a) clean hydroxylated silica; (b) silica reacted with DMZ in benzene solution, washed with dry benzene, evacuated at room temperature, and placed under nitrogen.

estimated to be $69 \pm 5\%$, similar to results seen by others.²³

Reaction of DMZ-Modified Silica Surface with n-Alkanethiols. *Chemical Vapor Deposition of EtSH on DMZ-Modified Silica.* Methane was detected in the gas-phase infrared spectra after exposing DMZ-pre-treated silica to a saturated vapor of EtSH at room temperature. The intensity of the $\sim 3016\text{ cm}^{-1}$ methane peak upon completion of the reaction is the same (~ 0.1 absorbance units) after initial reaction with DMZ and subsequent reaction with EtSH, suggesting that equal amounts of Zn-bound methyl species react at each step. Thermal evolution of the infrared spectra representing the new surface species formed after sequential exposure to DMZ and EtSH is shown in Figure 3. The assignments of the features are marked on the figure^{28,29} and correspond exactly to the modes of ethanethiolate species anchored to alumina.²¹ The $-\text{S}-\text{CH}_2-$ wagging mode, which is clearly seen in the case of the alumina substrate at $\sim 1262\text{ cm}^{-1}$, cannot be detected in this study because of the strong absorption of the Si–O lattice modes below 1300 cm^{-1} . A background experiment was conducted by exposing a clean hydroxylated silica surface directly to a saturated vapor of EtSH at room temperature. No residual surface species are detected, in accord with previous studies of thiol adsorption on alumina.^{21,30–32}

(29) Pouchert, Ch. *The Aldrich Library of Infrared Spectra*, 1975.

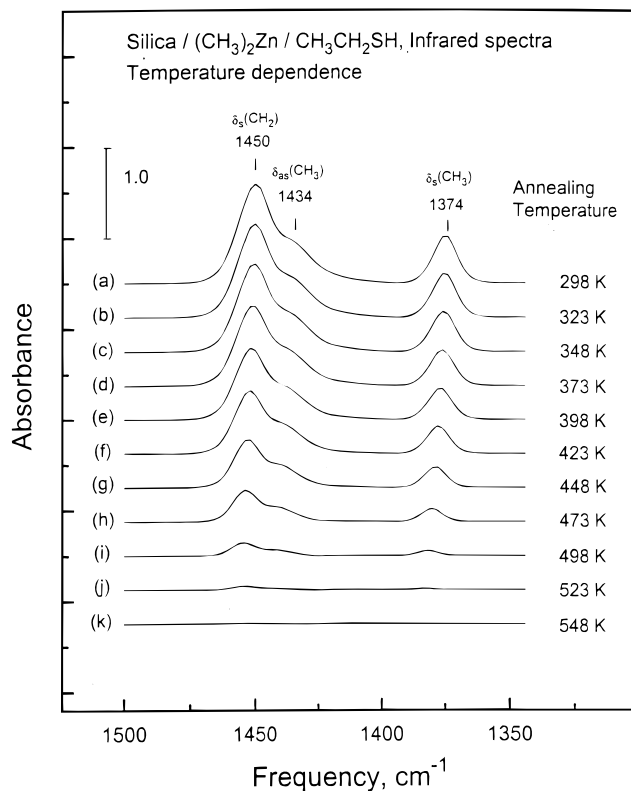


Figure 3. Bending region of baseline-corrected, temperature-dependent infrared spectra of a silica pellet modified by sequential chemical vapor deposition of DMZ and C_2H_5SH at room temperature and after annealing in vacuo at the temperature displayed adjacent to each spectrum.

These results suggest that most of the surface species remaining after prolonged evacuation at room temperature are reactively formed Zn-bound ethanethiolates. However, it is possible that some excess EtSH remains molecularly coordinated to the surface Zn centers, in addition to the reactively formed thiolates. In all spectra, a low-intensity infrared peak at $\sim 650\text{ cm}^{-1}$ is detected, which can be assigned to a C–S vibration.^{28,29}

All spectra shown in Figure 3 are obtained after annealing the modified silica pellet, first for ~ 30 min in the evacuated and closed infrared cell, to collect and monitor the gas-phase products evolved at each temperature, and then in vacuo for another ~ 30 min at the temperature displayed adjacent to each spectrum. The C–H bending modes gradually decrease in intensity, as estimated from the baseline-corrected, integrated infrared absorbance of $\delta_s(CH_2)$ and $\delta_{as}(CH_3)$ modes between 1478 and 1412 cm^{-1} , by $7 \pm 2\%$ in each annealing step up to 398 K [Figure 3(a–e)]. The first major loss of surface species occurs at 423 K [Figure 3(f)]. The amount remaining on the surface at 398 K [Figure 3(e)] is still $71 \pm 5\%$ of the initial coverage at room temperature [Figure 3(a)] and the amount lost at each subsequent 25 K temperature interval is nearly twice as large [$\sim 14\%$, Figure 3(f–i)], indicating a possible change in

the reaction pathway for adsorbate removal. Most of the species are lost by 523 K [Figure 3(j)].

The major products detected in the gas-phase infrared spectra are methane, EtSH diethyl sulfide, and ethylene. They are also observed during the thermal decomposition of Zn-bound ethanethiolate surface species on alumina.²¹ The temperature-dependent evolution of these products is evaluated using the intensity of their most distinct peaks at $\sim 3016\text{ cm}^{-1}$ for CH_4 ,³³ $\sim 1260\text{ cm}^{-1}$ for EtSH and diethyl sulfide,^{29,34} and $\sim 950\text{ cm}^{-1}$ for ethylene.³³ Because the most intense $-S-CH_2-$ wagging mode at $\sim 1260\text{ cm}^{-1}$ is common to both CH_3-CH_2SH and $(CH_3CH_2)_2S$, an attempt was made to use the frequency differences between their weaker skeletal modes²¹ to distinguish between these two products. Note that no diethyl disulfide was detected in any of the gas-phase infrared spectra. The final product of the thermal decomposition of these species may be infrared-transparent ZnS. This cannot be confirmed in this experiment, but is reported to be the final product from thermal decomposition of many thiolates.^{18,19,35–38}

Small amounts of methane (always less than $\sim 4\%$ of the intensity of the $\sim 3016\text{ cm}^{-1}$ peak observed after each of the deposition steps) are detected between 323 and 400 K and at temperatures higher than 500 K , and similar results were found for DMZ/EtSH-modified alumina.²¹ Very small amounts of CH_3CH_2SH desorb at 323 K , with increasing amounts of $(CH_3CH_2)_2S$ evolved between 348 and 423 K . Mostly $(CH_3CH_2)_2S$ is observed between 450 and 500 K . Ethylene is first detected at 448 K , reaches maximum intensity between 498 and 548 K , and gradually decreases to trace amounts at $\sim 598\text{ K}$.

To test the stability of the films, a DMZ+EtSH film was prepared and exposed to water vapor (20 Torr) for 7.5 h at room temperature. The baseline-corrected integrated absorbance between 1478 and 1412 cm^{-1} shows that only $13 \pm 2\%$ of the surface species initially present are lost upon exposure to water vapor. A small amount of methane is found in the gas phase. Almost no further methane is found, either upon exposure to air for $\sim 53\text{ h}$, or upon further heating at 323 K . The amount of species removed from the surface within the 323 – 448 K temperature interval at each annealing step in this experiment is similar to that found after annealing a sample not exposed to water or air.

Deposition of n-Alkanethiols of Various Chain Length on DMZ-Treated Silica from Benzene Solution. After DMZ reaction from solution illustrated by the infrared spectrum in Figure 2, the modified silica powder is thoroughly washed with fresh benzene and suspended in $\sim 5\text{ mL}$ of benzene. Then, an excess of the corresponding alkanethiol ($4 \times 10^{-3}\text{ mol}$) is added to the suspension. When the reaction is complete, the reactant

(30) Sugioka, M.; Kamanaka, T.; Aomura, K. *J. Catal.* **1978**, *52*, 531.

(31) Saur, O.; Chevreau, T.; Lamotte, J.; Travert, J.; Lavalley, J. C. *J. Chem. Soc., Faraday Trans. 1* **1981**, *77*, 427.

(32) Travert, J.; Saur, O.; Benaissa, M.; Lamotte, J.; Lavalley, J. C. In *Vibrations at Surfaces*; Caudano, R., Gilles, J. M., Lucas, A. A., Eds.; Plenum Press: New York, 1982; p 333.

(33) Herzberg, G. *Molecular Spectra and Molecular Structure, II. Infrared and Raman Spectra of Polyatomic Molecules*; D. Van Nostrand Co.: New York, 1947.

(34) Trotter, I. F.; Thompson, H. W. *J. Chem. Soc.* **1946**, 481.

(35) Osakada, K.; Yamamoto, T. *Inorg. Chem.* **1991**, *30*, 2328.

(36) Osakada, K.; Yamamoto, T. *J. Chem. Soc., Chem. Commun.* **1987**, 1117.

(37) Brennan, J. G.; Siegrist, T.; Carroll, P. J.; Stuczynski, S. M.; Reyniers, P.; Brus, L. E.; Steigerwald, M. L. *Chem. Mater.* **1990**, *2*, 403.

(38) Bochmann, M.; Webb, K. J. *Mater. Res. Soc. Symp. Proc.* **1991**, *204*, 149.

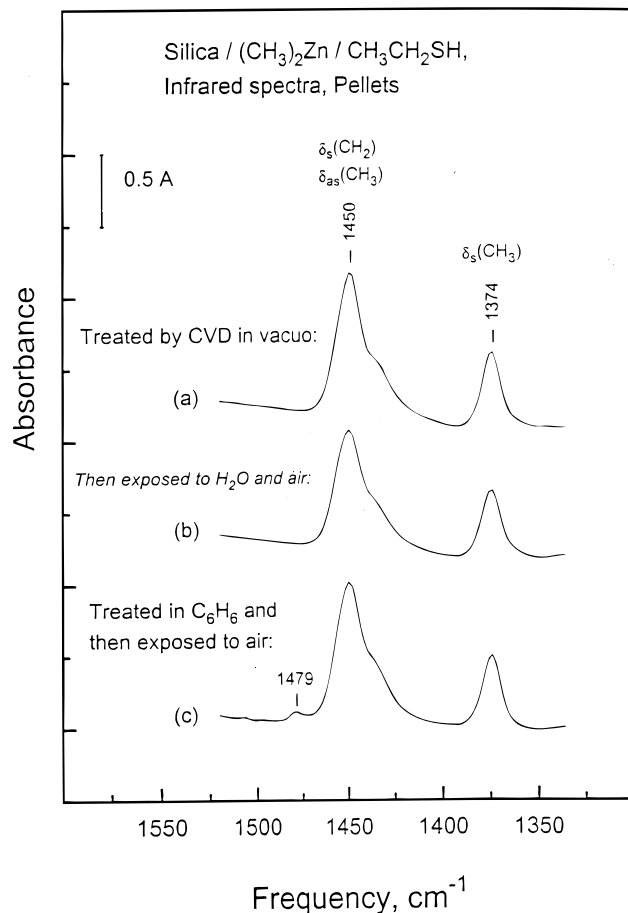


Figure 4. Comparison of infrared spectra obtained from silica surfaces modified by in vacuo sequential chemical vapor deposition of DMZ and EtSH [spectra (a) and (b)] and by sequential reaction in benzene [spectrum (c)].

solution is filtered out and the reacted silica thoroughly washed with fresh benzene, and vacuum-dried. The C–H bending region of an infrared spectrum taken from a silica pellet after sequential deposition of DMZ and EtSH from benzene solutions [Figure 4(c)] is compared with the spectra obtained from silica modified by reaction with vapor [Figure 4(a, b)]. The modes observed in the spectrum of the sample treated in benzene solutions are essentially identical to those found in the spectra of the vapor-treated sample. No significant change is observed upon exposing the silica modified in vacuo [Figure 4 (a)] to air [Figure 4 (b)]. The small feature at ~ 1479 cm^{-1} [Figure 4 (c)] is due to some traces of residual benzene.²⁸

The bending regions of the infrared spectra obtained from silica pellets, after solution deposition of DMZ and various thiols ($\text{C}_2\text{H}_5\text{SH}$, $\text{C}_4\text{H}_9\text{SH}$, or $\text{C}_8\text{H}_{17}\text{SH}$) in benzene, are shown in Figure 5. As the surface thiolate chain length increases, the frequency of their $\delta_s(\text{CH}_2)$ scissoring and symmetric methyl $\delta_s(\text{CH}_3)$ modes shifts slightly, with the most pronounced change observed between ethane [Figure 5 (a)] and butanethiolate [Figure 5(b)]. No significant change in the appearance of the bending modes is seen after prolonged refluxing of the DMZ-treated powder in octanethiol solution in benzene [Figure 5 (c–d)].

The C–H bending modes of longer-chain dodecanethiolate and hexadecanethiolate surface species on DMZ-

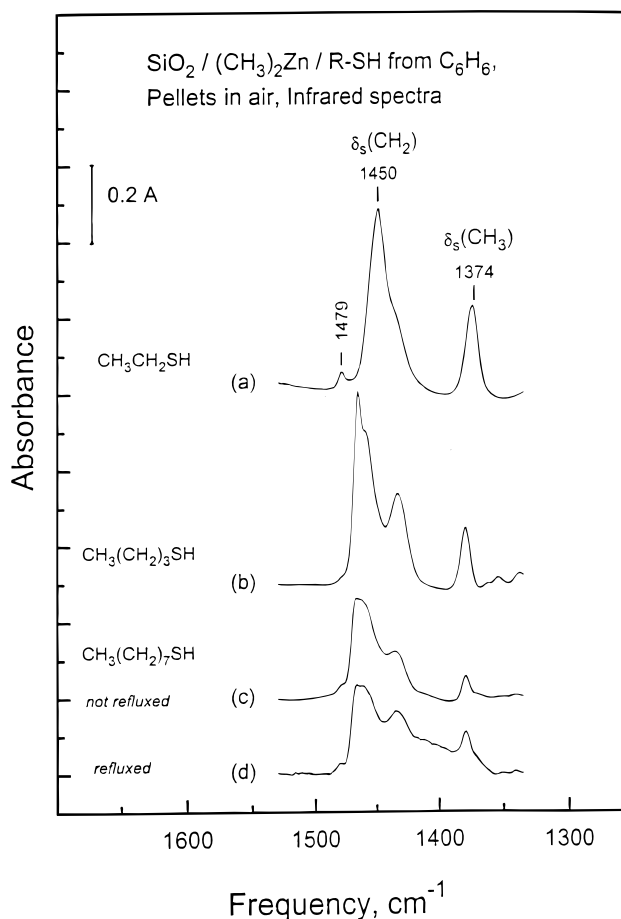


Figure 5. Bending region of the baseline-corrected infrared spectra of silica surfaces sequentially treated with DMZ and the corresponding thiol in benzene. Each sample is prepared by pressing the vacuum-dried modified powder into a pellet in air.

pretreated silica are shown in Figure 6. The higher intensity of the latter [Figure 6(a)] is due to the thicker sample. The C–H stretching region of these spectra is shown in Figure 7 (a, b), where the C–H stretching modes of hexadecanethiolate and dodecanethiolate surface species can be compared with those of the shorter surface thiolate chains [Figure 7 (c–e)]. The spectra in Figure 7 are not scaled because of the large difference in the layer thickness for each sample. All spectra in Figure 7 display asymmetric and symmetric methylene stretching modes at 2923 and 2852 cm^{-1} , together with the asymmetric and symmetric methyl stretching mode at 2957 cm^{-1} .

NMR Characterization. ¹³C NMR. The ¹³C–¹H CP MAS spectra of n-alkanethiols ($n = 2, 4, 8, 12,$ and 16) deposited on the modified silica surface are shown in Figure 8. Complete resolution of the signals from all nonequivalent carbon sites was obtained for the thiols with $n = 2$ and 4 ; for longer chains ($n = 8, 12,$ and 16) the signals from the inner CH_2 groups appeared as a single line. The assignment of the signals was made on the basis of comparison of these spectra with those obtained in solution.³⁹ Significant downfield chemical shifts and line broadening were observed for the carbons

(39) Sadtler Standard Carbon-13 NMR Spectra, Sadtler Research Laboratories, Editors and Publishers: 1995.

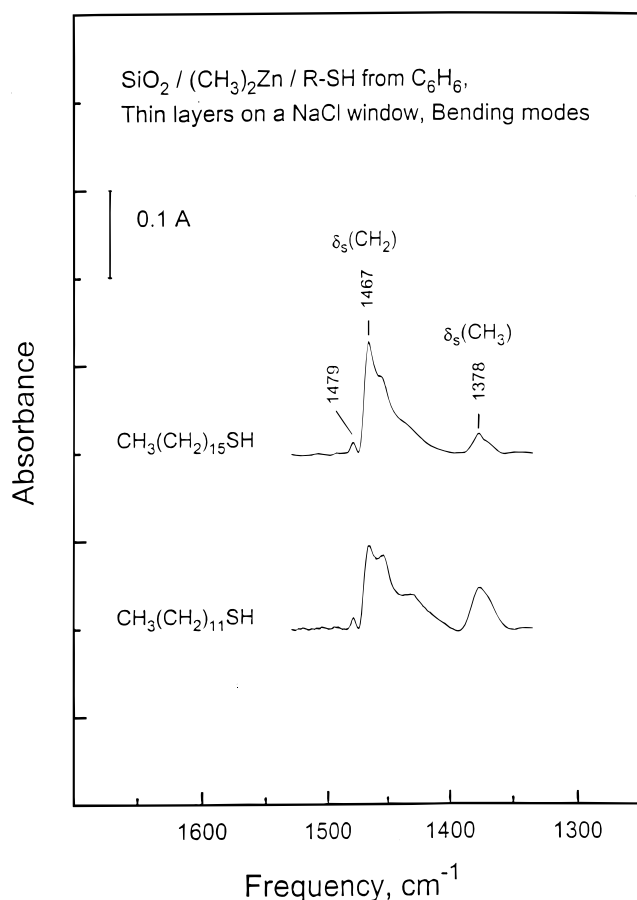


Figure 6. Bending region of baseline-corrected infrared spectra obtained from thin layers of silica powders modified by sequential treatment with DMZ and the corresponding thiol.

in the positions α and β (from the S center): $-\text{C}^{(\beta)}\text{H}_2-\text{C}^{(\alpha)}\text{H}_2-\text{S}-\text{Zn}-$. This effect is most probably due to the disordering interactions of the molecules with a surface. From these data it follows that the thiol chains interact with a surface without disproportionation and that they are oriented with sulfur toward the surface. The one-pulse ^{13}C NMR spectra with proton decoupling (not shown) reveal the same spectral patterns as the CP MAS spectra. No signals from methyl groups bound to Zn were observed.

The efficiency of the $^1\text{H} \rightarrow ^{13}\text{C}$ polarization transfer was unexpectedly quite uniform along the hydrocarbon chain; only in the case of long chains ($n = 12$ and 16) did the efficiency of the excitation of the terminal methyl carbon decrease slightly. This means that the reorientations of the methyl groups are not isotropic and rather hindered, so that the intramethyl dipolar interaction, which is responsible for the cross-polarization, is not averaged out. For example, the methyl groups in long-chain hydrocarbon surfactants used in the synthesis of mesoporous solids are not visible in $^{13}\text{C}-^1\text{H}$ CP MAS spectra.⁴⁰

Additional evidence for the specific interaction of the $-\text{C}^{(\alpha)}\text{H}_2-\text{S}-\text{Zn}-$ fragment with the surface was found in the case of $\text{C}_4\text{H}_9\text{SH}$ thiol (Figure 9). In the $^{13}\text{C}-^1\text{H}$

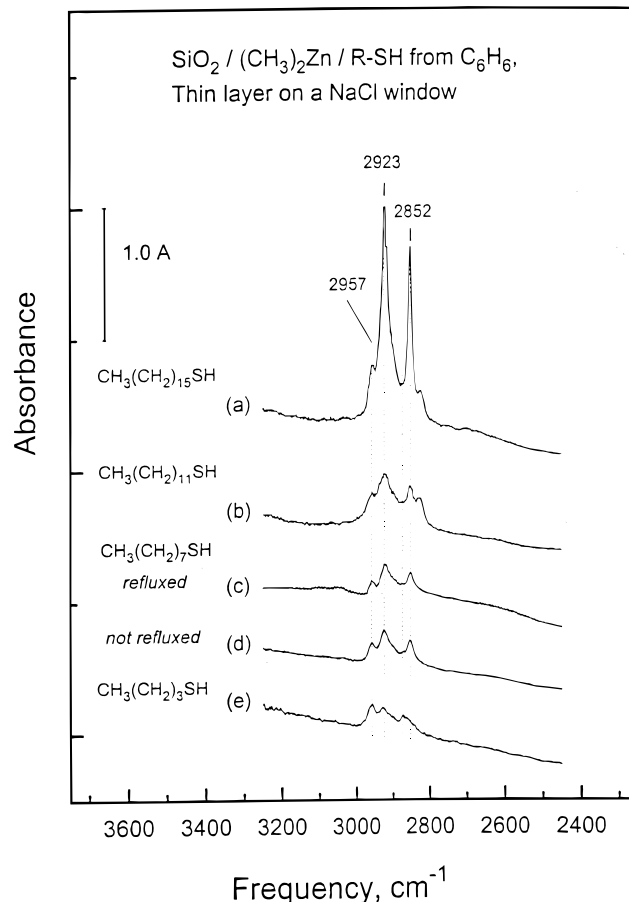


Figure 7. Stretching region of the infrared spectra obtained from thin layers of silica powders sequentially treated in benzene with DMZ and the corresponding thiol.

CP MAS spectra of this thiol on the modified silica surface all four signals are well-resolved and assigned. The 10-fold decrease in the proton decoupling power did not change the line widths of the carbons in positions 3 and 4. However, the broadening of the line assigned to the carbon in position 1 is quite pronounced (see Table in Figure 9). This broadening is, of course, due to the dipolar coupling of the $\text{C}^{(\omega)}$ carbon with the surface OH groups; this coupling could not be averaged out by MAS at the moderate rate (4 kHz) used in this experiment.

²⁹Si NMR. The one-pulse ²⁹Si NMR spectra of all samples reveal the same pattern: two signals at ~ 110 and ~ 100 ppm with the ratio 3:1 (Figure 10). These signals are usually assigned to the ⁴Q and ³Q silicon species.⁴¹ The ⁴Q are tetrahedral Si sites with four silicon neighbors in the first coordination sphere; the ³Q are the sites lacking one silicon in the first sphere. It is reasonable to assume that only ³Q-type silicons provide sites for adsorption.

The $^1\text{H}-^{29}\text{Si}$ CP MAS provides more information on the interaction between thiol chains and the silica surface. The two sites, ³Q and ⁴Q, are distinguished not only by their different chemical shifts, but also by the strength of the dipolar interactions with the protons of the organic species (the heteronuclear dipolar interaction is inversely proportional to the cube of the internuclear distances). We have investigated the cross-

(40) Beck, J. S.; Vartuli, J. C.; Roth, W. J.; Leonowicz, M. E.; Kresge, C. T.; Schmitt, K. D.; Chu, C. T.-W.; Olson, D. H.; Sheppard, E. W.; McCullen, S. B.; Higgins, J. B.; Schlenker, J. L. *J. Am. Chem. Soc.* **1992**, *114*, 10834.

(41) Engelhardt, G.; Michel, D. *High-Resolution Solid-State NMR of Silicates and Zeolites*; Wiley: New York, 1987.

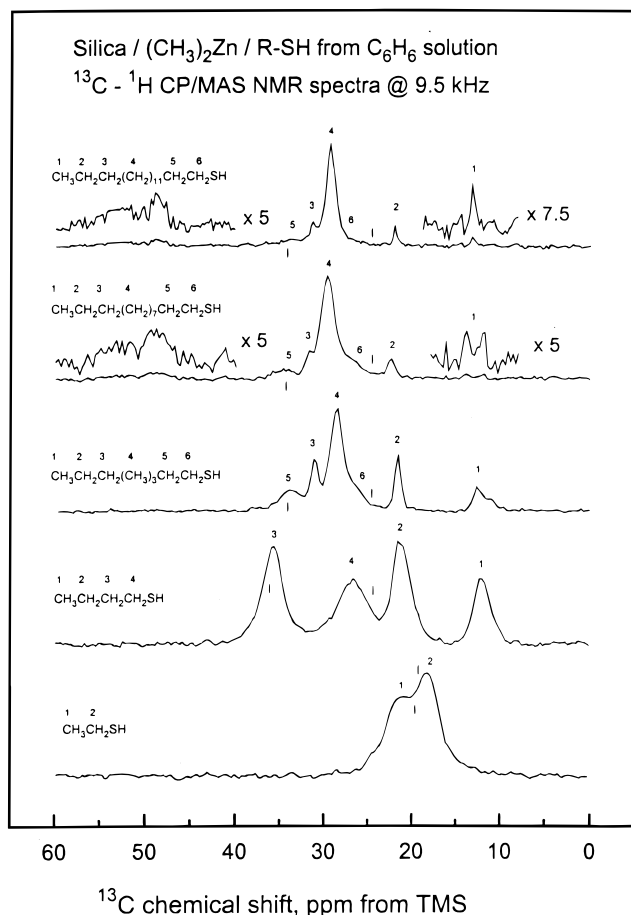


Figure 8. ^{13}C - ^1H CP/MAS NMR spectra of high-surface-area silica powder sequentially reacted with DMZ and *n*-alkanethiols. Assignments of the different carbon atoms from the grafted surface species are made according to ref 39 by comparison with spectra obtained from the corresponding liquid thiols. The chemical shifts of the two carbons adjacent to the sulfur in the spectrum of each *liquid thiol* are marked on the correspondent spectrum from the modified silica powder to show the change of width and position due to interactions of grafted hydrocarbon chains with silica surface.

polarization dynamics between surface silicons and the protons of the organic layer. In these experiments the magnetic polarization is transferred from protons (excited nuclei) to nearby silicons (observed nuclei). We have studied the dynamics of the polarization transfer to two distinct Si sites on the surface: of Q_4 type (110 ppm) and of Q_3 type (100 ppm). To increase the selectivity of the experiments, we performed an additional study using a predeuterated sample in which the source of the polarization is solely due to the organic layer. Figure 10 shows the evolution of the ^1H - ^{29}Si CP MAS spectra of the butanethiol adsorbed on the protonated (Figure 10A) and on the deuterated (Figure 10B) surface with increasing values of contact time. The different behavior of both sites on different surfaces is clearly seen. The plots in Figure 10 were obtained by the fitting procedure described in the Experimental Section. Table 1 gives the data obtained for the butanethiol sample. There are two time constants involved in the dynamics of the magnetization transfer, $T_{1\rho}$ (proton relaxation) and T_{CP} (cross-relaxation). The latter parameter provides structural information, because it is inversely proportional to the sum $\sum 1/r_i^6(\text{Si}-\text{H}_i)$. The T_{CP} time constant for the ^3Q site

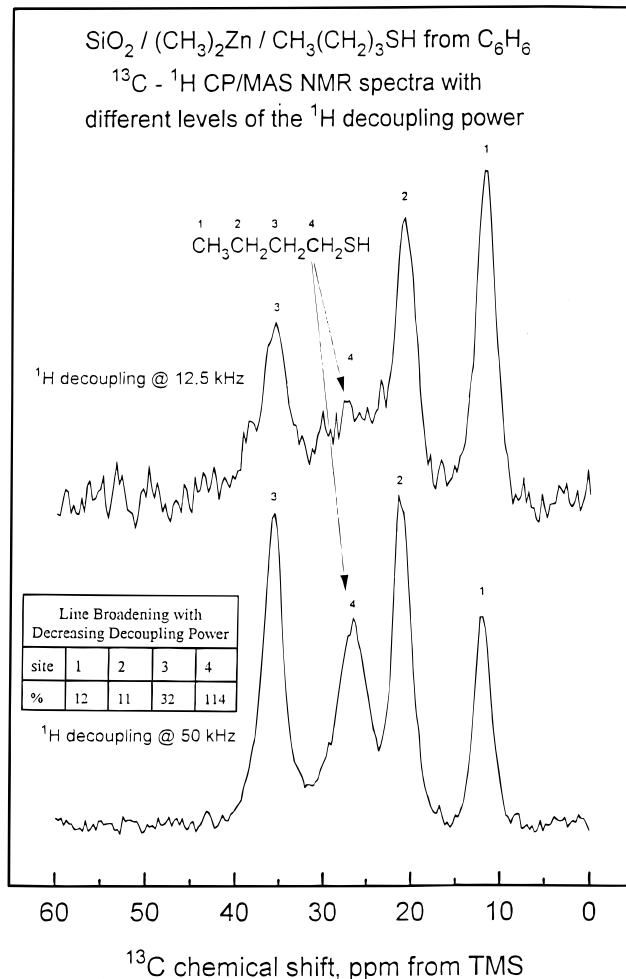


Figure 9. ^{13}C - ^1H CP/MAS spectra of the surface species grafted on silica by sequential reaction with DMZ and *n*-butanethiol in benzene; bottom trace: strong ^1H decoupling power; top trace: weak ^1H decoupling power.

on the deuterated surface is about 5 times larger than the value obtained for the protonated surface. Assuming that, on the deuterated surface, the surface silicons are solely dipolar coupled with the protons of the adsorbed butanethiol, one can roughly estimate the Si-C⁽¹⁾ internuclear distance. For this purpose the CP dynamics data for systems with known geometry are needed. In previous studies of the polarization transfer between silicons and chemisorbed ammonia in mordenite zeolite,⁴² the T_{CP} time constant was 2.4 ms. The rough estimate (see ref 24), taking into account the different numbers of protons and different rotational dynamics of the protons in the two systems, suggests that the ratio $r[\text{Si}-\text{C}^{(1)}, \text{butanethiol on silica}]/r[\text{Si}-\text{NH}_4^+, \text{ammonia on mordenite}] \approx 1.75 \pm 0.25$.

Elemental Analyses. The average thiolate coverage on the modified silica samples was estimated for each sample from the total carbon content obtained from CHN elemental analyses (Figure 11). The results clearly show that the thiolate coverage decreases significantly with increasing hydrocarbon chain length. This may be attributed to a steric effect related to the irregular porous structure of the high-surface-area silica powder

(42) Blumenfeld, A.; Coster, D.; Fripiat, J. *J. Phys. Chem.* **1995**, *99*, 15181.

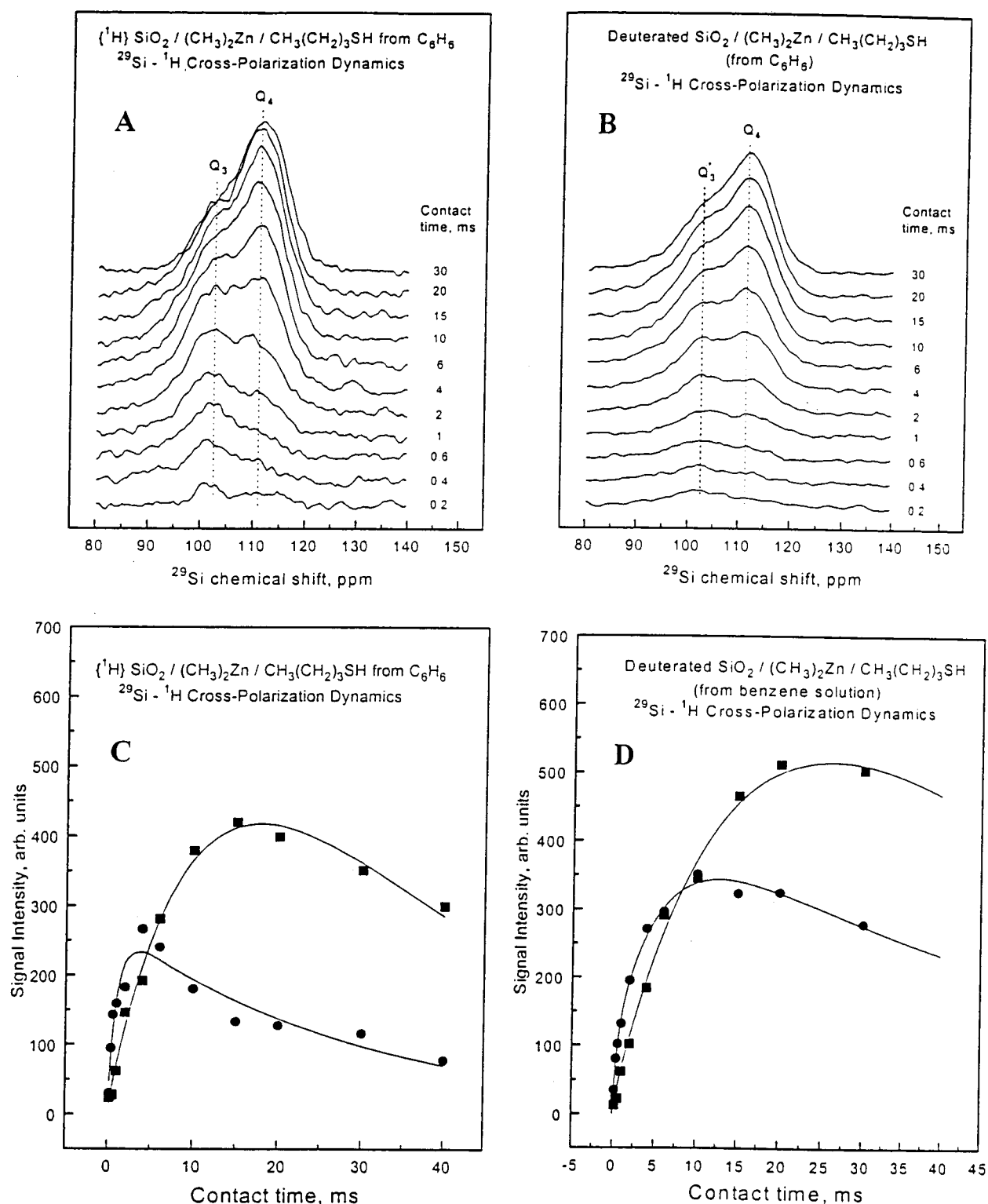


Figure 10. ^1H - ^{29}Si cross-polarization spin dynamics in DMZ/*n*-butanethiol-modified silica powder treated in benzene. CP/MAS spectra with various contact times: (A) protonated surface; (B) deuterated surface. The time evolution of the ^4Q (■) and ^3Q (●) versus contact time: (C) protonated surface; (D) deuterated surface.

or to a decrease in reactivity of the thiols with increasing chain length. Note that the ethanethiolate coverage estimated from the total carbon content ($\sim 9.5 \times 10^{14}$ chains/ cm^2 , Figure 11) is within the same order of magnitude as that of the densely packed alkyltrichlorosilane-derived self-assembled monolayers on planar silicon surfaces [$\sim 5 \times 10^{14}$ chains/ cm^2 (ref 5, p 108)]. One of the octanethiolate samples was treated at room

temperature and the other had been additionally refluxed for a few hours in the reactant solution. The difference in total octanethiolate coverage of these samples is well within the error of the measurement. Additional experiments were conducted by varying the refluxing time, but no significant differences in the thiolate coverages were found. This implies that the decreasing thiolate coverage found with increasing

Table 1: ^{29}Si - ^1H Cross-Polarization Spin Dynamics in DMZ/*n*- $\text{C}_4\text{H}_9\text{SH}$ -Modified Silica

| | $\text{CH}_3(\text{CH}_2)_3\text{S}$ -: cross-polarization dynamics | | | |
|--------------------------------|---|--------------|--------------|--------------|
| | deuterated | | protonated | |
| | Q_4 | Q_3 | Q_4 | Q_3 |
| rel. int. | 3.1 | 1 | 3.0 | 1 |
| T_{H}^{H} , ms | 34.7 | 34.7 | 27.3 | 26.9 |
| T_{CP} , ms | 19.3 | 5.8 | 11.3 | 1.1 |

Time-constants and relative intensities were obtained by deconvolution of the spectra displayed in Figure 15 (A) and (B) and fitting the integral intensities with eq 1 in the Experimental Section.

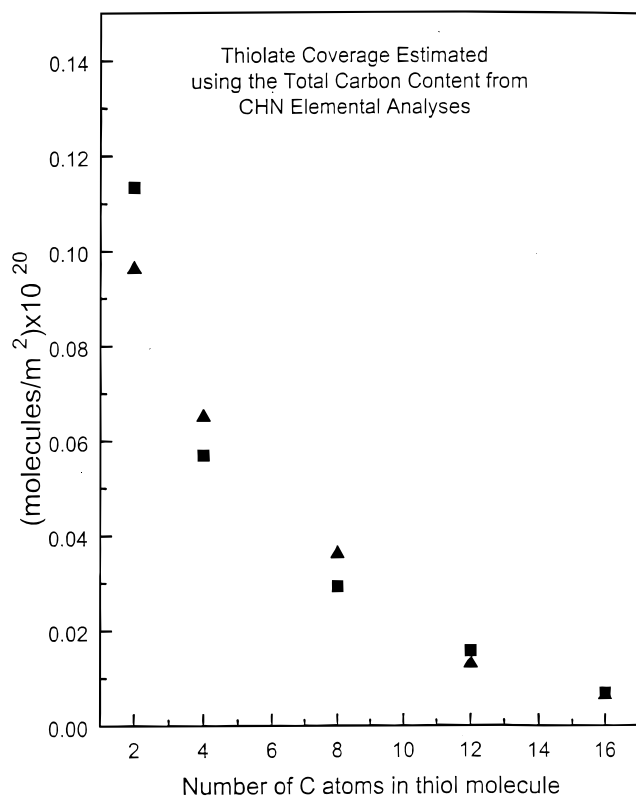


Figure 11. Thiolate coverage of silica samples sequentially reacted with DMZ and the corresponding *n*-alkanethiol as a function of hydrocarbon chain length. Total carbon content from CHN analysis has been normalized to the number of carbon atoms in the thiol molecule and coverage is estimated using the Brunover–Emett–Teller surface area of the clean hydroxylated silica.

hydrocarbon chain length is primarily due to steric effects. It should be emphasized that self-assembly of the hydrocarbon chains is not to be expected on such a high-surface-area, microporous substrate.

CHN elemental analysis was also used to verify that no hexadecanethiol(ate) remains on the silica surface after direct treatment in benzene solution without DMZ modification of the surface under the same other conditions.

Electron microprobe elemental analysis (EDS) was used to measure the sulfur and zinc content of the surface-modified silica powders. The results displayed in Figure 12 confirm the trend of decreasing thiolate coverage derived from the CHN data (Figure 11) because every S atom on the modified surface directly represents a grafted thiolate species. The Zn content is reasonably constant for all samples. The estimated S/Zn

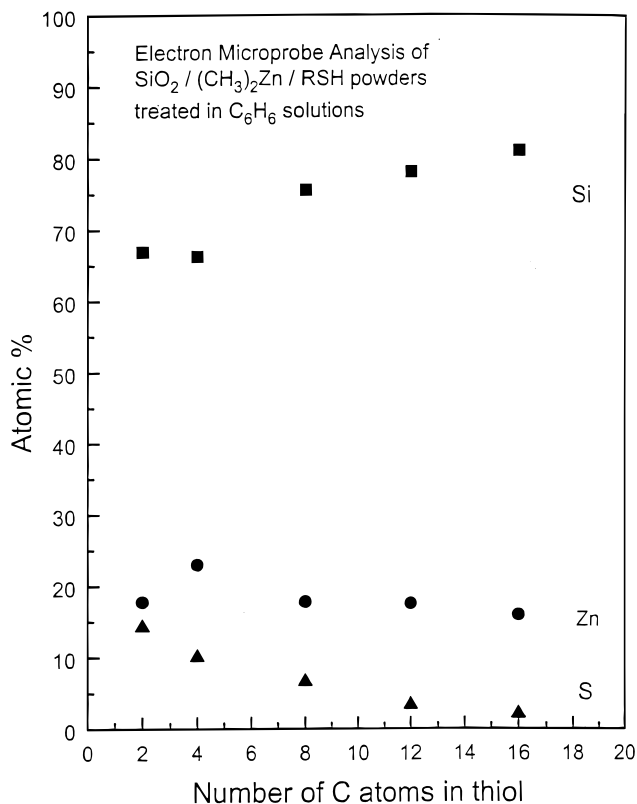


Figure 12. Sulfur (\blacktriangle), zinc (\bullet) and silicon (\blacksquare) content of silica powders modified by sequential reaction with DMZ and *n*-alkanethiols in benzene measured by electron microprobe (EDS) elemental analysis and displayed as a function of the hydrocarbon chain length of the grafted thiol.

ratio for a DMZ/EtSH-treated sample is ~ 0.8 , which confirms that a small number of Zn- CH_3 surface species is not accessible even for the shortest-chain EtSH molecules. The decreasing sulfur content with increasing thiol chain length, while the Zn content remains relatively constant, again emphasizes that not all of the Zn sites may be available for thiol adsorption. Some of them may be blocked by the irregular silica surface or the anchored thiolate chains.

These results show that alkanethiols react with a DMZ-modified hydroxylated silica surface according to the pathway shown in Scheme 1. This is confirmed because equimolar amounts of methane are evolved in each reaction step. In addition, methyl species are detected on the surface after exposure to DMZ vapor (Figure 1) and from solution (Figure 2). Exposure to the EtSH grafts strongly bound thiolate species on the surface (Figure 3), and this chemistry is in accord with that previously found on alumina.²¹

This vapor-phase chemistry can also be implemented from solution, as confirmed by the following observations:

(1) Identical high-intensity infrared C-H bending modes are observed in the spectra of DMZ/EtSH-modified silica samples, prepared both by chemical vapor deposition in vacuo and from benzene solutions (Figure 4).

(2) Dense ethanethiolate coverages [estimated from the CHN elemental analysis (Figure 11)] are obtained in benzene solution that are within the range of well-

ordered self-assembled monolayers formed from trichlorosilanes.

(3) Results from electron microprobe analysis of DMZ+EtSH-modified samples reveal similar sulfur and zinc contents (Figure 12)

(4) There was no thiol adsorption on silica surfaces not pretreated by DMZ.

These observations confirm that DMZ reacts both in vacuo and in benzene according to Scheme 1.

The results from NMR spectroscopy clearly demonstrate that all alkanethiolate chains retain their integrity and do not undergo any secondary chemical transformations other than methane elimination from the reactive thiol group and surface methylzinc species because no side products were detected from any of the modified silica samples (Figure 8–10). This further confirms that the alkanethiolate chains are bound to the surface via their reactive sulfur-containing headgroups. In addition, the NMR experiments demonstrate that the tails of the surface thiolate species point away from the surface.

These results indicate that organic films can be grown on silica by sequential reaction of DMZ and an alkanethiol from solution and that these films are stable in air and aqueous environments (Figure 6).

Conclusions

DMZ reacts with surface silanols to evolve methane to form mainly monomethylzinc surface species. These

can further react with n-alkanethiols of various chain length ($C_2 - C_{16}$) to eliminate methane and anchor Zn-bound alkanethiolate species to the silica surface. These are stable in air and in aqueous environments. Almost identical results are obtained when these reactions are carried out in vacuo using chemical vapor deposition and in benzene solutions with EtSH. This indicates that this modification strategy can be implemented both in vacuo using short-chain thiols with high vapor pressure and in organic solutions using longer-chain thiols to develop a novel method for preparation of self-assembled monolayers on different planar hydroxylated solid surfaces. On high-surface-area silica, the amount of surface alkanethiolate species grafted from benzene solutions using this reaction sequence significantly decreases with increasing chain length. This effect is independent of the reaction temperature and is attributed to the steric limitations of the irregular high-surface-area powders, which may be avoided by using planar substrates. Anchored thiolate chains are bound to the surface Zn sites by their reactive sulfur-containing headgroups, and their tails are pointed away from the surface, indicating the suitability of this strategy for self-assembly on planar hydroxylated surfaces.⁴³

CM000083I

(43) Koeck, B. W.; Kleisner, R. J.; Phillips, M. J.; Wieland, J. A.; Gutow, J. A.; Boiadjev, V.; Tysoe, W. T., in press.